Review TRENDS in Biochemical Sciences Vol.29 No.8 August 2004

Energy transduction in transmembrane ion pumps

Marc T. Facciotti[1], Shahab Rouhani-Manshadi[2] and Robert M. Glaeser[3]

[1]Institute for Systems Biology, 1441 North 34th Street, Seattle, WA 98103, USA
[2]Donner Laboratory, Lawrence Berkeley National Laboratory, University of California, Berkeley, CA 94720, USA
[3]Department of Molecular and Cell Biology, and Donner Laboratory, Lawrence Berkeley National Laboratory, University of California, Berkeley, CA 94720, USA

Recent crystallographic structures of three different ion pumps provide a first view of the mechanisms by which these molecular machines transfer ions across cell membranes against an electrochemical gradient. Each of the structures reinforces the concept that several buried counter ions have central roles in substrate recruitment, substrate binding and energy transduction during ion pumping. The spatial organization of the counter ions suggests that, initially, one or more counter ions lowers the Born energy cost of binding a substrate ion in the low-dielectric interior of the membrane. Subsequently, a ligand-induced conformational change seems to close a charged access gate to prevent backflow from a subsequent, low-affinity state of the pump. A final role of the buried counter ions might be to couple the input of external energy to a small charge separation between the substrate ion and the buried counter ions, thereby decreasing the binding affinity for the substrate ion in preparation for its release on the high-energy side of the membrane.

Membrane pumps carry out a diverse set of biochemical functions, including the import of small organic molecules needed for fuel or biosynthesis, the maintenance of ionic gradients and membrane potentials, and the expulsion of various intruding, xenobiotic molecules. The engineering challenges that must be solved in the design of a membrane pump are similar to those encountered in a boat lock in a canal (Figure 1). Unlike the familiar, macroscopic boat lock, however, a membrane pump must work autonomously and, like any other enzyme, membrane pumps must be built from a set of no more than 20 universal components. Advances in the crystallography of membrane proteins are now beginning to identify the molecular designs of a few such membrane pumps [1–12], revealing the nature of previously abstract concepts such as molecular gates, openings and closings, and intramembrane ion-binding sites. The structures provide us with opportunities to understand the physical mechanisms by which these membrane pumps work.

Ion pumps require that their design must define a reaction coordinate for the transport of substrate that avoids the formidable Born energy barrier (Box 1). The design of gated ion channels must also overcome the Born energy problem, of course, and design solutions that achieve this are known for several ion channels from X-ray crystallography [13–18]. As we explain below, however, it now seems that, despite the apparent functional similarity (ion channels transport ions across a lipid bilayer), a design that is well-suited for an ion channel, or perhaps even a secondary active transporter [19], might not be adequate to fulfill the additional requirements of a membrane pump.

X-ray crystallography of bacteriorhodopsin and several of its mutants including the anion-pumping Asp85Ser mutant, bR(D85S), has advanced rapidly in recent years [20]. This structural data set represents the most extensive collection of such information that is available for any single ion pump. Thus, insights gained from this set of structures have now been combined to provide a first glimpse of the design by which at least one particular membrane protein carries out all of the requirements of an ion pump. One should recognize, however, that each type of ion pump might have unique biochemical, thermodynamic and structural characteristics.

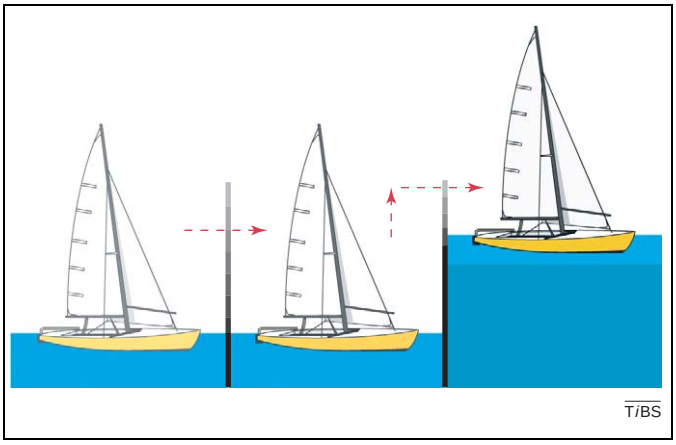

Figure 1. The cycle of operations in a membrane pump must be fundamentally similar to that in a boat lock in a canal. Both machines are designed to transport a substrate from a region of low potential energy to a region of high potential energy. In this cartoon of a boat lock, both the boat and the sluice gates are shown with changing transparency to indicate their motion as the cycle of operations advances. Once the boat (substrate) has entered the lock (binding pocket), the entry gate must close so that the boat (substrate) will not flow backwards after external energy has been used to lift it to a higher energy level. After a high-energy (low-affinity) state has been generated, the exit gate must open to release the boat (substrate) to the opposite side. After transport (translocation) of the boat (substrate), the machine must be returned to its initial configuration so that the cycle can be repeated again.

Corresponding author: Robert M. Glaeser (rmglaeser@lbl.gov).

Box 1. The energy-cost of burying an ion pair

It is energetically unfavorable to move an ion from a medium with a high dielectric constant (ε), such as water, to a medium with a low dielectric constant, for example, the middle of a lipid bilayer or the interior of a protein. The physical basis for the energy difference can be understood in terms of a 'continuum-dielectric model', first invoked by Born [49], in which the energies needed to charge a conducting sphere in the two media are calculated. According to this model, the energy (ΔU) needed to move an ion from water, where $\varepsilon=80$, into an environment with a low dielectric constant is

$$\Delta U = q^2/2a(1/\varepsilon - 1/80)$$

where q is the charge of the ion and a is its radius. Despite the obvious weakness of applying a continuum-dielectric model to the atomic scale of ions and their surrounding molecules, the values of ionic radii, a, that give good agreement with experimental transfer energies correspond well to the physical radii of various ions. As a representative calculation, the cost of burying an ion of radius $a=2$ Å in a medium with $\varepsilon=2$ is estimated to be about 40 kcal mol^{-1}.

When two ions with similar radii but opposite charge are buried in a medium of low dielectric constant, it is energetically favorable for them to form an ion pair, as indicated in Figure I. Because the centers of the ions will be separated by a distance of $2a$, the energy released by formation of an ion pair will be

$$\Delta U' = -q^2/2\varepsilon a$$

To an accuracy of 1–2%, therefore, we can say that the favorable energy of forming an ion pair completely compensates for the unfavorable energy of burying the second ion [45,46]. In other words, if the cost of burying an initial counter ion can be paid in some way, then doing so will then prepay the subsequent cost of burying a substrate ion.

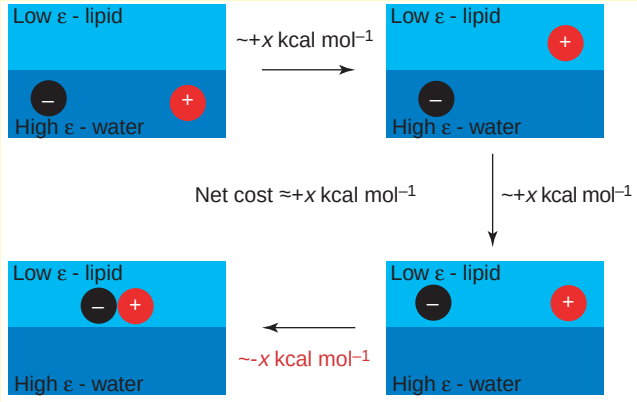

Figure I. Cartoon showing how the initial cost of burying a fixed counter ion in a medium of low dielectric constant will prepay the subsequent cost of burying an ionic substrate in the same medium. Although the combined cost of burying both ions is represented as being '2x' kcal mol^{-1} (x being dependent, of course, on the value of the ambient dielectric constant), the formation of an ion pair recovers an energy of x kcal mol^{-1} that is virtually the same as the cost of burying one ion – taken here to be the cost of burying the substrate ion.

Nevertheless, as we describe below, a comparison of the structural information that is available for bacteriorhodopsin, an anion-pumping mutant of bacteriorhodopsin, halorhodopsin and the Ca^{2+}-ATPase reveals common principles for coping with the Born energy barrier and for gating access to the internal binding site that are likely to be of general importance.

Experimental description of bacteriorhodopsin

The bacteriorhodopsin photocycle generates a proton-motive force [21,22] over a wide range of ambient pH values. When Asp85 is protonated at low pH, however, the wild-type protein acts as a Cl^- ion pump [23], as does its homologous membrane protein, halorhodopsin, under physiological conditions [24]. Indeed, when Asp85 is replaced by the polar but uncharged residues threonine or serine, the resulting single-mutant proteins also function as Cl^- ion pumps [25–27]. These observations thus suggest that although wild-type bacteriorhodopsin is widely considered to be a proton pump, it might be more parsimonious to propose that it is actually a hydroxyl ion pump [28].

The protein fold of bacteriorhodopsin is perhaps the most familiar fold of all membrane proteins. Electron crystallography was the first technique to show, at moderate resolution, that the polypeptide chain forms seven transmembrane helices that are bundled together in an essentially elliptical cylinder [29]. Subsequent X-ray crystallographic work at more than 2 Å resolution has further sharpened the precision with which we now know the structure of this protein [1,30–32].

Remarkably, the deprotonated carboxyl groups of Asp85 and Asp212 are buried close to the protonated Schiff base formed by all-*trans* retinal and the ε-amino group of Lys216. Along with the buried guanidinium group of Arg82, these residues form a complex counter ion assembly deep within the extracellular half of the membrane. These structural features are conserved in halorhodopsin [3], with the functionally important exception that threonine replaces Asp85 on the extracellular side of the protein.

The earliest two intermediates in the bacteriorhodopsin photocycle (K and L) form on timescales of picoseconds and microseconds, respectively. Not surprisingly, little structural change is shown by the protein within such short time intervals [1,33–35]. Instead, it is likely that the energy of the absorbed photon introduces elastic strain in the molecule through photoisomerization of the retinal chromophore. A cascade of structural substates is then generated over a timescale from a few microseconds to about 10 milliseconds, during which both the Schiff base and the carboxyl group of Asp85 are neutralized, producing the yellow form of the protein known as the 'M intermediate' [36]. At the same time, the elastic strain caused earlier by the shortening (13-*cis* isomerization) of the retinal prosthetic group is relaxed by a shift in the position of the backbone of Lys216, which in turn is accommodated by a concerted switch in hydrogen bonding in one turn of the π-helix in helix G [37]. Part of the energy released in this structural relaxation can be mechanically coupled to perform the work that is required for substrate movement.

High-resolution X-ray crystal structures have not yet captured the outward tilt of the cytoplasmic side of helix F that is known – from lower resolution electron diffraction studies [38–42] – to occur in the late M and N phases of the pumping cycle. Presumably, crystal packing forces in the three-dimensional crystals deny the protein access to this conformation, which is readily adopted by bacteriorhodopsin in the two-dimensional crystals used for electron diffraction studies. The latter represent a condition that most closely resembles the *in vivo* functional arrangement

of the wild-type protein. The repacking of the helices on the cytoplasmic side of the protein during the N-like portion of the pumping cycle is likely to correspond functionally to formation of the cytoplasmically open conformation postulated in Jardetzky's model of membrane pumps [43].

The final intermediate in the photocycle, known as the 'O intermediate', has proved to be the most difficult one to trap in the native membrane [44]. Fortunately, however, bR(D85S) can be considered to be constitutively in an O-like state when not bound to anion. The high-resolution X-ray crystal structure of this mutant shows the presence of an 'opening' of the helices on the extracellular side of the protein [45]. Several hydrogen-bond interactions between the helices are rearranged on the extracellular side of this mutant, and even the centers of most of the helices are shifted from the positions adopted in the resting state of the wild-type protein. If we refer again to the boat lock analogy, the O intermediate might therefore correspond to the initial configuration of the boat lock shown in Figure 1, with the binding site open to access from the extracellular side of the membrane.

Anion binding in the bR(D85S) mutant and halorhodopsin

Binding of a substrate anion by bR(D85S) produces a complex arrangement of counter ions that resembles the arrangement found in the wild-type protein [2,28]. It is therefore not surprising that anion binding also induces a repacking of helices on the extracellular side of the protein that brings their hydrogen-bond interactions and tertiary structure closer to that of the resting state of bacteriorhodopsin. Substrate binding thus seems to induce an autonomous conformational change that closes the previously open entry gate to prevent backflow of substrate. As is true for a boat lock, it is especially important that backflow is prevented before an external source of energy is used to raise the potential of the substrate.

Both Br^- ions and NO_3^- ions can bind in the same binding pocket of bR(D85S), where they make a direct ion pair interaction with the protonated Schiff base. Both anions also interact with the hydroxyl group of Ser85 (although this residue adopts a slightly different rotamer conformation in each case), as well as with the protonated form of Asp212 (Figure 2a,b). In the absence of a bound anion, the same site is occupied by a water molecule [45], as it is in the wild-type protein [1,30–32]. The native Cl^- ion pump, halorhodopsin, binds its substrate ion in a homologous site (Figure 2c). In all cases where an anion occupies the binding site, the side chain of Arg82 (and the equivalent residue in halorhodopsin, Arg108) is found to be in an upward-facing conformation, as it is in the resting state of wild-type bacteriorhodopsin.

The Born energy for substrate binding is prepaid by buried counter ions

It makes intuitive sense for the substrate-binding site of a membrane pump to be located at a relatively deep, internal site of the protein [3,4,11,12,46]. For an ion pump, however, this design poses a potential problem in terms of the high energy cost of burying the substrate ion in a low-dielectric environment. As explained further in Box 1, however, the formation of an ion pair between the substrate ion and a previously buried counter ion gives back the same amount of energy as it costs to bury the substrate ion initially [47,48]. The energetic cost of burying the fixed counter ion itself, in turn, can be paid during protein folding by burial of the large, hydrophobic surface of a transmembrane helix [49]. Additional, buried polar groups and even buried water molecules contribute further to creating a favorable binding site deep in the interior of the protein.

The design strategy of using buried counter ions to prepay the Born energy cost is also adopted by Ca^{2+}-ATPase. This protein buries at least five carboxyl side chain residues (Figure 2d), which in turn form a complex counter ion network with two Ca^{2+} ions in the Ca^{2+}-bound state of the pump [4]. Additional 'solvation' of the bound ions is provided by polar side chain residues and by carbonyl groups from a short, non-helical part of the

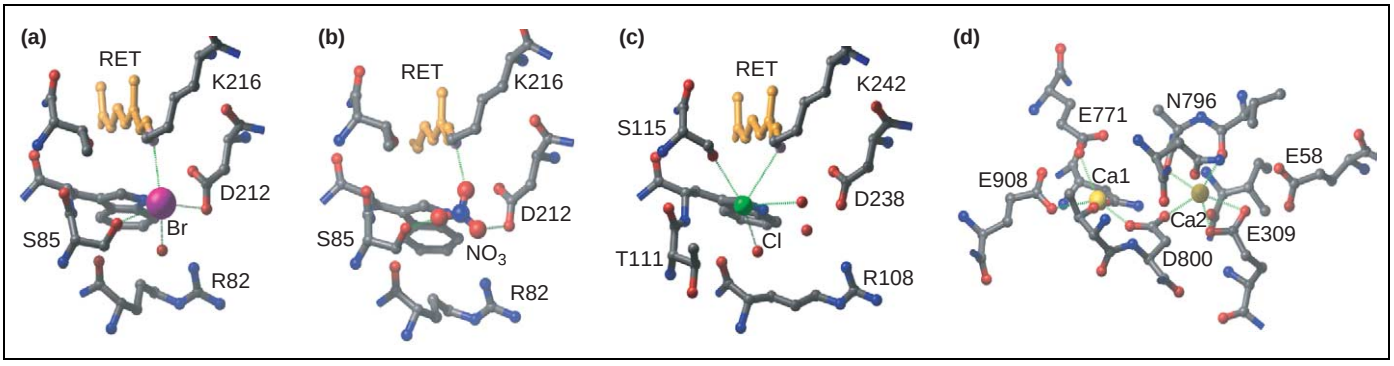

Figure 2. The binding sites in three different ion pumps each feature buried, charged groups that make ion pairs with the substrate ion. **(a)** Br^- ion binding in the bacteriorhodopsin anion-pumping mutant bR(D85S) [2]. The Br^- ion makes an ion pair with the protonated Schiff base. In addition, the ion is 'solvated' by hydroxyl groups from Ser85, the protonated form of Asp212, and a buried water molecule. **(b)** NO_3^- ion binding in bR(D85S) [56]. One oxygen atom of the NO_3^- ion makes an ion pair with the protonated Schiff base, while the other two oxygen atoms each participate in the formation of hydrogen bonds with the hydroxyl groups of Ser85 and the protonated form of Asp212, respectively. The larger size of the NO_3^- anion precludes the inclusion of a buried water molecule in the binding pocket in this case. **(c)** Cl^- ion binding in halorhodopsin [3]. The Cl^- ion is located below the protonated Schiff base and is directly solvated by two water molecules and the side chain oxygen of Thr111. These interactions are highlighted by broken lines. A complex hydrogen-bonding network (not shown), including a third water molecule and Arg108, further stabilize the binding of Cl^-. **(d)** Ca^{2+} ion binding in the Ca^{2+}-ATPase [4]. Two Ca^{2+} ions are bound in the active site. Each cation is directly associated with two carboxyl side chain residues. Additional solvation is provided by backbone and side chain atoms. In the crystal structure, no ordered water molecules are found to be involved in Ca^{2+} binding in the cation-bound resting state. Abbreviation: RET, retinal.

polypeptide backbone – a strategy similar to the one adopted by ion channel proteins.

At this point, one might wonder why not all of the Born energy is prepaid by 'solvating' the substrate ion with the dipoles of peptide groups in ion pumps, as occurs in ion channels. We return to this point further below, when we discuss a strategy that seems to use charge separation within the ion pair to couple the consumption of energy to the task of raising the electrochemical potential of the substrate ion. For now, we re-emphasize only the fact that ion pumps seem to solve the Born energy problem in a markedly different way from the approach that is used by ion channels [13–18].

Access to the internal binding pocket is controlled by a counter ion

In the anion-bound state of halorhodopsin [3], as well as in the anion-bound state of bR(D85S) [2], there is no solvent-accessible tunnel that connects the binding site to the aqueous surface of the pump. Instead, access to the binding site is physically blocked by a conserved arginine residue (Figure 3a,b), as it is in the resting state of wild-type bacteriorhodopsin (not shown). What is surprising, however, is the fact that there still is no solvent-accessible tunnel that extends into the binding site in the anion-free form of bR(D85S) (Figure 3c), even though the helices on the extracellular side have been repacked in what seems to be a more open conformation [45].

Because in bR(D85S) the side chain of Arg82 still blocks access to the binding site in the anion-free pump, one must postulate that the substrate anion gains access to the protein interior as a result of dynamic fluctuations in the protein structure. Indeed, the concept of a 'flickering gate' was suggested previously to explain the dynamics of ion release in both the sarcoplasmic reticulum Ca^{2+}-ATPase [50] and the Na^{+}/K^{+}-ATPase [51]. In addition, such a concept, supported by molecular dynamics simulations, has been proposed to explain how molecular oxygen is able to reach its heme-group-binding site in myoglobin [52]. A switch from the 'open' to the 'closed' state of a membrane pump might therefore involve a change only in how easily the ever-present fluctuations in protein structure can enable the substrate to pass through to, or from, an internal binding site – a possibility that was anticipated by Jardetzky [43] in his conceptual model of membrane pumps.

When the substrate is an ion, however, a membrane pump must provide more than just a transient opening for the substrate to pass into the internal binding site. Penetration of an ion only as far as 0.5 nm into a low-dielectric medium already encounters a very high Born energy barrier [47,53,54]. As a result, the design of an ion pump must provide a solution for the Born energy problem right at the mouth of the access site, and not just at the internal binding site. The guanidinium group of arginine is well suited to function as a 'Born energy chaperone' or dynamic gate (Figure 3a,b) that again prepays the Born energy cost, but this time for transport of the substrate ion into its proper binding site [2].

In halorhodopsin, Arg108 (homologous to Arg82 of bacteriorhodopsin) has been postulated by Kolbe *et al.* [3] to function in substrate recruitment. In the Ca^{2+}-ATPase, it seems that Glu309, which blocks physical access to the internal substrate-binding sites (Figure 3d), might have a similar role in substrate recruitment for this ion pump. On the one hand, in all pumps the chaperone counter ion should only lower the barrier of the transition between the 'inside' and the 'outside' by providing an electrostatic partner for the substrate: it should not trap the ion in a deep potential well. On the other hand, additional binding partners available to the ion in the binding site, as compared with the more limited interactions postulated to occur in the area of the chaperone, should produce a more stable minimum along the reaction coordinate.

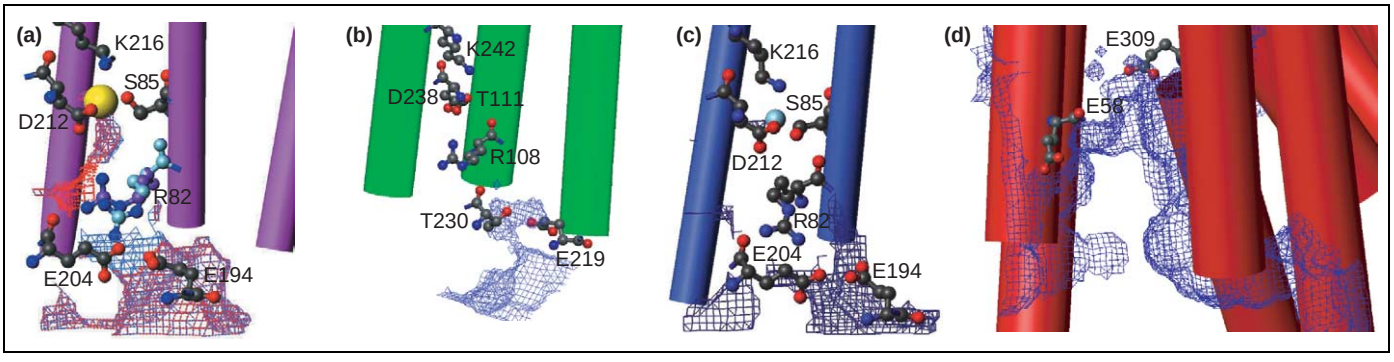

Figure 3. The access gate between the substrate-ion-binding site and the solvent-accessible surface of the membrane pump is closed when the substrate ion is in its binding pocket. **(a)** Ion-bound state of the bacteriorhodopsin anion-pumping mutant bR(D85S) [2]. The rotamer conformation of Arg82 is in an upward-facing conformation, in which the guanidinium group blocks access to and from the binding pocket even for a water molecule. The two conformations of Arg82 modeled in this structure are indicated with their representative solvent-accessible surfaces shown as blue and red wire. Because key helix–helix interactions on the extracellular side of the membrane are similar to those found in wild-type bacteriorhodopsin [1,30–32], we propose that the side chain of Arg82 is no longer free to swing between the upward-facing and downward-facing states, and thus the access gate is essentially in a closed, locked state. **(b)** Ion-bound state of halorhodopsin [3]. The side chain of Arg108 blocks solvent-accessible access to the ion-binding site in halorhodopsin and, as in bacteriorhodopsin, the rotamer conformation of this residue is in an upward-facing state, suggesting that it participates in the delivery of substrate into the binding site. The solvent-accessible tunnel is shown as blue wire. **(c)** Ion-free state of bR(D85S) [45]. A water molecule occupies the ion-binding site in the absence of a bound anion. The side chain of Arg82 is now in a downward-facing rotamer conformation, suggesting that it has a role in forming an ion pair with a substrate anion to lower the energy barrier for entering the low-dielectric interior of the protein. The solvent-accessible tunnel is shown as blue wire. **(d)** Ion-free state of Ca^{2+}-ATPase [5]. The side chain of Glu309 blocks solvent-accessible access to the ion-binding site and adopts a downward-facing rotamer conformation. In the cation-bound structure of this ion pump, Glu309 adopts an upward-facing rotamer conformation, which, along with large-scale helical rearrangements, blocks entry or exit to the binding site, reminiscent of the way in which arginine side chains do the same thing in bR(D85S) and possibly in halorhodopsin. The solvent-accessible tunnel is shown as blue wire. Parts (a) and (c) reproduced, with permission, from Ref. [2].

Box 2. Molecular designs of ion pumps

A first glimpse of the active transport of ions across cell membranes can be best assembled from the extensive crystal structures of bacteriorhodopsin and several its mutants, most notably the anion pump bR(D85S). Similar details are also evident in the less-complete structural data available for Ca^{2+}-ATPase and halorhodopsin, a naturally occurring Cl^- ion pump.

As shown in Figure I, the ion pump begins its cycle with its internal binding site 'open' to one side of the membrane, as indicated by the broadened shape of the bottom half of the protein. At this stage, no continuous, solvent-accessible tunnel is open in either bR(D85S) or Ca^{2+}-ATPase. As a result, it is likely that access to the binding site must be afforded by dynamic fluctuations of the structure, the possibility of which is indicated by the wavy line from the binding site to the bottom of the protein.

Fixed counter ions seem to prepay the Born energy cost associated with burying the substrate ion both while it is in transit to the binding pocket and when it is bound in the resting state. Binding of ligand – an anion in bR(D85S) – then induces a change in protein conformation that 'closes' the gate. In bR(D85S), halorhodopsin and Ca^{2+}-ATPase, it seems that the previously dynamic counter ion, which originally mediated entry to the binding site, might become locked in an immobilized conformation as a result of the repacking of helices that occurs when substrate is bound. This step is indicated in Figure I by a change in the shape of the bottom half of the protein and by a transition from a wavy line to a straight line between the bottom of the protein and the anion-binding pocket.

The coupling of external energy, which is an essential aspect of active transport, seems to occur in the form of a small separation between the counter ion and the substrate ion in the binding pocket. Because even a small amount of charge separation consumes a large amount of energy, it is likely that the substrate ion will follow the forced movements of the counter ion as closely as possible, even if doing so requires breaking other interactions with polar, 'solvating' groups in the binding pocket. The net result is that the substrate ion is lifted to a state of higher potential energy.

The creation of a high-energy state of the pump must also result in the 'opening' of a pathway for the substrate ion to escape on the opposite side of the membrane. The transient formation of such an inward-facing photointermediate has been observed in electron diffraction studies of both wild-type bacteriorhodopsin and two different mutants of bacteriorhodopsin [36–40]. A similar protein conformation is seen constitutively in the bR(D96G/F171C/F219L) triple mutant [53]. This part of the ion-pumping cycle remains the least well-characterized state for all of the known ion pumps. As a result, little can be said about the molecular events that release the substrate ion from its low-affinity state into the aqueous environment on the opposite side of the membrane, where its chemical potential remains high. Similarly, as yet no structural information can explain how the release of the substrate from its low-affinity state results in the protein returning to its initial, ligand-free conformation.

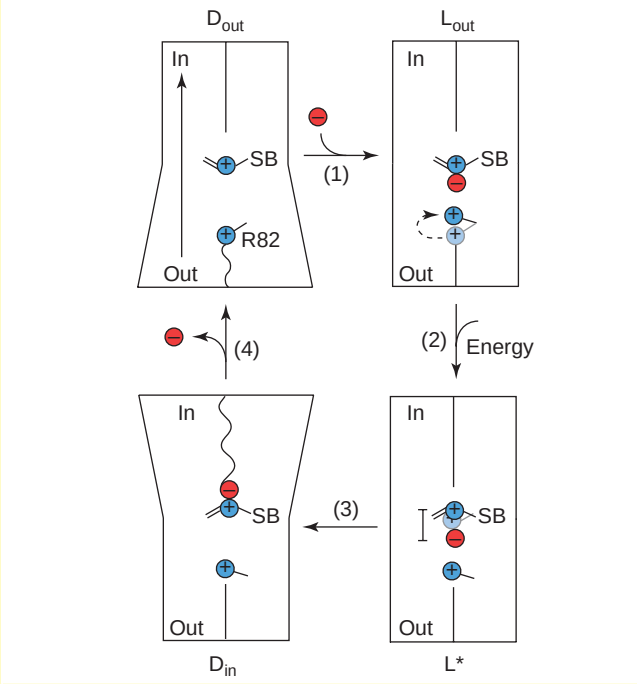

Figure I. Cartoon summarizing the known atomic details of how bR(D85S) works as an ion pump. The substrate anion (red sphere) and the Schiff base linkage to the retinal (SB) are indicated. The direction of pumping, from the outside into the cytosol, is indicated by the arrow in the first panel (top left). The four states shown in this simplified cycle are as follows: D_{out} is capable of 'dynamic opening' in the outward (bottom) half of the pump; in L_{out}, the access gate in the outward half of the pump is 'locked'; L^* is a high-energy (low-affinity) state in which the access gate must remain 'locked'; and D_{in} is capable of 'dynamic opening' in the inward half of the pump. Modified, with permission, from Ref. [2].

Charge separation is likely to raise the potential of ionic substrates

Because as yet there is no high-resolution crystal structure of a photoproduct of the anion-bound bR(D85S) mutant, we can construct only a preliminary model of how photoisomerization is likely to raise the energy of the anionic substrate in the binding pocket. We feel that it is reasonable to assume that the reaction coordinate for the photocycle of the anion-bound mutant protein, when expressed in structural terms, cannot change substantially owing to the substitution of serine for aspartate at position 85. We have therefore used the crystal structure of a late-M intermediate [37] to model a likely structure of the photoproduct of anion-bound bR(D85S).

Alignment of the resting-state structure of the Br^--bound bR(D85S) mutant and the late-M photoproduct of the bR(D96N) mutant (Figure 4) indicates that the distance between the Br^- ion and the midpoint of the N–H bond of the protonated Schiff base is likely to increase by at least 40% relative to the corresponding

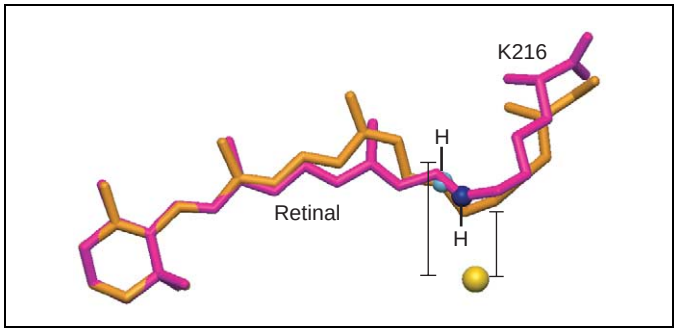

Figure 4. The initial energy that accompanies photoisomerization of the retinal group in the bacteriorhodopsin anion-pumping mutant bR(D85S) seems to be coupled to a rise in the chemical potential of the substrate anion through a forced, partial separation of the ion pair that the substrate makes with the protonated Schiff base of the retinal group. To model what is likely to occur, the structure of a late-M intermediate of bacteriorhodopsin has been aligned to the resting state of bR(D85S) with a Br^- ion in the binding pocket [2]. The bars between the Br^- ion (yellow sphere) and the midpoint of the N–H bond of the protonated Schiff base give an indication of the amount of charge separation that would occur if the Br^- ion did not move from its resting-state position. Reproduced, with permission, from Ref. [2].

distance in the resting state [2]. According to this rough model, therefore, the work needed to produce what seems to be only a very small charge separation would be as much as 40% of the work needed to separate the two charges to infinity.

Depending on whether we take the dielectric constant for the environment of the ion pair to be 2 or 4, the electrostatic potential for the substrate ion will be increased by roughly 10 or 20 kcal mol^{-1}. This increase in the electrochemical potential of the substrate ion is still a relatively small fraction of the energy of a photon (50 kcal mol^{-1} for 570-nm photons), but it is more than enough to pump an ion against a thousand-fold concentration difference, against a transmembrane potential of 100 mV, or even against both at the same time. There is good reason, thus, to propose that having a buried counter ion in the substrate-binding pocket serves two purposes. First, the use of a buried counter ion provides a good solution to the Born energy problem when the substrate ion is initially bound deep in the membrane. Second, a subsequent step of partial separation of the counter ion from the substrate ion provides a good mechanism by which to couple the consumption of externally supplied energy to the required increase in the electrochemical potential of the substrate.

As has been discussed in considerable detail by Stokes and Green [55], it seems that even larger rearrangements of counter ions and substrate ions occur in the interior binding pocket of the Ca^{2+}-ATPase. Still missing in this story, however, are crucial high-resolution structures of the phosphorylated protein and the protein in various states involving bound nucleotide. Nevertheless, a comparison of the substrate-free [5] and substrate-bound [4] structures of the Ca^{2+}-ATPase reveals a large solvent-accessible tunnel leading from the cytoplasmic surface towards the binding site. This tunnel terminates short of the actual binding pocket, however, on the downward-oriented, negatively charged side chain of Glu309. Furthermore, it seems that another residue, Glu58, which forms a wall of the binding site, also points downward towards the cytosol at the end of the solvent-accessible tunnel. We speculate that these two residues act in concert to chaperone the divalent Ca^{2+} ion into the binding site. Binding of the Ca^{2+} ions (substrate ions) also induces a very large conformational change on the cytoplasmic side of the protein, which is likely to act, at least in part, to close the gate on the cytoplasmic side of the protein.

The model of energy coupling that we have described for opsin pumps is, however, still too simplistic. It is physically unreasonable to suppose that the substrate ion would remain stationary such that photoisomerization could produce the amount of charge separation that we have modeled between the Schiff base and the substrate anion. Instead, we can expect the substrate anion to move along with the protonated Schiff base to maintain a stronger ion pair complex. The substrate ion could do this, however, only at the expense of giving up some of the other, favorable 'solvation' interactions that are described in Figure 2a. Thus, by moving away from other polar groups within the binding pocket, the substrate ion would remain at a relatively high chemical potential, in other words, in a lower affinity state.

Concluding remarks

We have discussed recent advances in the macromolecular crystallization of transmembrane ion pumps and have shown how these structures both provide a detailed understanding of the molecular nature of previously abstract concepts, such as gates, intramembrane binding sites, and open and closed conformations, and suggest new concepts such as that of 'Born energy chaperones'.

Specifically, the structural information that is now available for bacteriorhodopsin and some of its mutants has been used to construct a model (Box 2) of the complete pumping cycle for the bacteriorhodopsin anion-pumping bR(D85S) mutant. This construction is based on the assumption that point mutations that retain an ion-pumping photocycle do not change the basic reaction coordinate, when expressed in structural terms, that is followed after light is absorbed by the retinal prosthetic group.

As a result, several principles have been reaffirmed regarding the operation of the anion-pumping bR(D85S) mutant, and it is possible that these same principles might be used by other ion pumps. In support of such a suggestion of generality, we can identify similar design principles that are adopted by the Ca^{2+}-ATPase pump and, not surprisingly, by halorhodopsin – a halide-pumping protein that is homologous to bacteriorhodopsin.

Note added in proof

Two new crystal structures for the Ca^{2+}-ATPase appeared [57] while this review was in proof. These structures add information about the rather large conformational change that occurs (i) when a nonhydrolyzable ATP analog is bound (a change that is described as closing the door against Ca^{2+}-substrate backflow) and (ii) the very small, but important, further structural change that occurs upon binding a presumed transition state analog for the formation of the high-energy phosphorylated intermediate (a structural change that is described as locking the door after it had been closed).

Acknowledgements

This work has been supported, in part, by a grant (GM51487) from the National Institutes of Health.

References

1 Schobert, B. *et al*. (2002) Crystallographic structure of the K intermediate of bacteriorhodopsin: conservation of free energy after photoisomerization of the retinal. *J. Mol. Biol.* 321, 715–726
2 Facciotti, M.T. *et al*. (2003) Crystal structure of the bromide-bound D85S mutant of bacteriorhodopsin: principles of ion pumping. *Biophys. J.* 85, 451–458
3 Kolbe, M. *et al*. (2000) Structure of the light-driven chloride pump halorhodopsin at 1.8 Å resolution. *Science* 288, 1390–1396
4 Toyoshima, C. *et al*. (2000) Crystal structure of the calcium pump of sarcoplasmic reticulum at 2.6 Å resolution. *Nature* 405, 647–655
5 Toyoshima, C. and Nomura, H. (2002) Structural changes in the calcium pump accompanying the dissociation of calcium. *Nature* 418, 605–611
6 Stock, D. *et al*. (1999) Molecular architecture of the rotary motor in ATP synthase. *Science* 286, 1700–1705

7 Chang, G. and Roth, C.B. (2001) Structure of MsbA from *E. coli*: a homolog of the multidrug resistance ATP binding cassette (ABC) transporters. *Science* 293, 1793–1800
8 Locher, K.P. *et al*. (2002) The *E. coli* BtuCD structure: a framework for ABC transporter architecture and mechanism. *Science* 296, 1091–1098
9 Murakami, S. *et al*. (2002) Crystal structure of bacterial multidrug efflux transporter AcrB. *Nature* 419, 587–593
10 Yu, E.W. *et al*. (2003) Structural basis of multiple drug-binding capacity of the AcrB multidrug efflux pump. *Science* 300, 976–980
11 Abramson, J. *et al*. (2003) Structure and mechanism of the lactose permease of *Escherichia coli*. *Science* 301, 610–615
12 Huang, Y. *et al*. (2003) Structure and mechanism of the glycerol-3-phosphate transporter from *Escherichia coli*. *Science* 301, 616–620
13 Doyle, D.A. *et al*. (1998) The structure of the potassium channel: molecular basis of K^+ conduction and selectivity. *Science* 280, 69–77
14 Zhou, Y.F. *et al*. (2001) Chemistry of ion coordination and hydration revealed by a K^+ channel-Fab complex at 2.0 Å resolution. *Nature* 414, 43–48
15 Jiang, Y. *et al*. (2002) Crystal structure and mechanism of a calcium-gated potassium channel. *Nature* 417, 515–522
16 Jiang, Y. *et al*. (2003) X-ray structure of a voltage-dependent K^+ channel. *Nature* 423, 33–41
17 Zhou, Y. and MacKinnon, R. (2003) The occupancy of ions in the K^+ selectivity filter: charge balance and coupling of ion binding to a protein conformational change underlie high conduction rates. *J. Mol. Biol.* 333, 965–975
18 Dutzler, R. *et al*. (2002) X-ray structure of a ClC chloride channel at 3.0 Å reveals the molecular basis of anion selectivity. *Nature* 415, 287–294
19 Accardi, A. and Miller, C. (2004) Secondary active transport mediated by a prokaryotic homologue of ClC Cl^- channels. *Nature* 427, 803–807
20 Cartailler, J.P. and Luecke, H. (2003) X-ray crystallographic analysis of lipid–protein interactions in the bacteriorhodopsin purple membrane. *Annu. Rev. Biophys. Biomol. Struct.* 32, 285–310
21 Oesterhelt, D. and Hess, B. (1973) Reversible photolysis of the purple complex in the purple membrane of *Halobacterium halobium*. *Eur. J. Biochem.* 37, 316–326
22 Racker, E. and Stoeckenius, W. (1974) Reconstitution of purple membrane vesicles catalyzing light-driven proton uptake and adenosine triphosphate formation. *J. Biol. Chem.* 249, 662–663
23 Der, A. *et al*. (1991) Alternative translocation of protons and halide ions by bacteriorhodopsin. *Proc. Natl. Acad. Sci. U. S. A.* 88, 4751–4755
24 Schobert, B. *et al*. (1983) Evidence for a halide-binding site in halorhodopsin. *J. Biol. Chem.* 258, 15158–15164
25 Sasaki, J. *et al*. (1995) Conversion of bacteriorhodopsin into a chloride ion pump. *Science* 269, 73–75
26 Brown, L.S. *et al*. (1996) Interaction of proton and chloride transfer pathways in recombinant bacteriorhodopsin with chloride transport activity: Implications for the chloride translocation mechanism. *Biochemistry* 35, 16048–16054
27 Kalaidzidis, I.V. and Kaulen, A.D. (1997) Cl^--dependent photovoltage responses of bacteriorhodopsin: comparison of the D85T and D85S mutants and wild-type acid purple form. *FEBS Lett.* 418, 239–242
28 Facciotti, M.T. *et al*. (2004) Crystal structures of bR(D85S) favor a model of bacteriorhodopsin as an hydroxyl-ion pump. *FEBS Lett.* 564, 301–306
29 Henderson, R. *et al*. (1990) Model for the structure of bacteriorhodopsin based on high-resolution electron cryo-microscopy. *J. Mol. Biol.* 213, 899–929
30 Luecke, H. *et al*. (1999) Structure of bacteriorhodopsin at 1.55 Å resolution. *J. Mol. Biol.* 291, 899–911
31 Belrhali, H. *et al*. (1999) Protein, lipid and water organization in bacteriorhodopsin crystals: a molecular view of the purple membrane at 1.9 Å resolution. *Structure Fold. Des.* 7, 909–917
32 Facciotti, M.T. *et al*. (2001) Structure of an early intermediate in the M-state phase of the bacteriorhodopsin photocycle. *Biophys. J.* 81, 3442–3455
33 Lanyi, J. and Schobert, B. (2002) Crystallographic structure of the retinal and the protein after deprotonation of the Schiff base: the switch in the bacteriorhodopsin photocycle. *J. Mol. Biol.* 321, 727–737
34 Lanyi, J.K. and Schobert, B. (2003) Mechanism of proton transport in bacteriorhodopsin from crystallographic structures of the K, L, M1, M2, and M2′ intermediates of the photocycle. *J. Mol. Biol.* 328, 439–450
35 Edman, K. *et al*. (2004) Deformation of helix C in the low temperature L-intermediate of bacteriorhodopsin. *J. Biol. Chem.* 279, 2147–2158
36 Betancourt, F.M. and Glaeser, R.M. (2000) Chemical and physical evidence for multiple functional steps comprising the M state of the bacteriorhodopsin photocycle. *Biochim. Biophys. Acta* 1460, 106–118
37 Luecke, H. *et al*. (1999) Structural changes in bacteriorhodopsin during ion transport at 2 Angstrom resolution. *Science* 286, 255–260
38 Subramaniam, S. *et al*. (1993) Electron diffraction analysis of structural changes in the photocycle of bacteriorhodopsin. *EMBO J.* 12, 1–8
39 Han, B.G. *et al*. (1994) The bacteriorhodopsin photocycle: direct structural study of two substrates of the M-intermediate. *Biophys. J.* 67, 1179–1186
40 Vonck, J. *et al*. (1994) Two progressive substrates of the M-intermediate can be identified in glucose-embedded, wild-type bacteriorhodopsin. *Biophys. J.* 67, 1173–1178
41 Hendrickson, F.M. *et al*. (1998) Structural characterization of the L-to-M transition of the bacteriorhodopsin photocycle. *Biophys. J.* 75, 1446–1454
42 Vonck, J. (2000) Structure of the bacteriorhodopsin mutant F219L N intermediate revealed by electron crystallography. *EMBO J.* 19, 2152–2160
43 Jardetzky, O. (1966) Simple allosteric model for membrane pumps. *Nature* 211, 969–970
44 Subramaniam, S. *et al*. (1997) Electron diffraction studies of light-induced conformational changes in the Leu-93→Ala bacteriorhodopsin mutant. *Proc. Natl. Acad. Sci. U. S. A.* 94, 1767–1772
45 Rouhani, S. *et al*. (2001) Crystal structure of the D85S mutant of bacteriorhodopsin: model of an O-like photocycle intermediate. *J. Mol. Biol.* 313, 615–628
46 Hirai, T. *et al*. (2002) Three-dimensional structure of a bacterial oxalate transporter. *Nat. Struct. Biol.* 9, 597–600
47 Parsegian, A. (1969) Energy of an ion crossing a low dielectric membrane: solutions to four relevant electrostatic problems. *Nature* 221, 844–846
48 Honig, B.H. and Hubbell, W.L. (1984) Stability of 'salt bridges' in membrane proteins. *Proc. Natl. Acad. Sci. U. S. A.* 81, 5412–5416
49 Steitz, T.A. *et al*. (1982) Quantitative application of the helical hairpin hypothesis to membrane proteins. *Biophys. J.* 37, 124–125
50 Orlowski, S. and Champeil, P. (1991) Kinetics of calcium dissociation from its high-affinity transport sites on sarcoplasmic reticulum ATPase. *Biochemistry* 30, 352–361
51 Forbush, B., III. (1987) Rapid release of 42K or 86Rb from two distinct transport sites on the Na,K-pump in the presence of Pi or vanadate. *J. Biol. Chem.* 262, 11116–11127
52 Karplus, M. and McCammon, J.A. (1986) The dynamics of proteins. *Sci. Am.* 254, 42–51
53 Born, M. (1920) Volumen und hydataionswaerme der ionen. *Z. Phys.* 1, 45–48
54 Glaeser, R.M. and Jap, B.K. (1984) The 'Born Energy' problem in bacteriorhodopsin. *Biophys. J.* 45, 95–96
55 Stokes, D.L. and Green, N.M. (2003) Structure and function of the calcium pump. *Annu. Rev. Biophys. Biomol. Struct.* 32, 445–468
56 Facciotti, M.T. *et al*. (2004) Specificity of anion-binding in the substrate-pocket of bacteriorhodopsin. *Biochemistry* 43, 4934–4943
57 Sorensen, T.L. *et al*. (2004) Phosphoryl transfer and calcium ion occlusion in the calcium pump. *Science* 304, 1672–1675